

Bootstrap Segmentation Foundation Model under Distribution Shift via Object-Centric Learning

Luyao Tang^{1*}, Yuxuan Yuan^{1*}, Chaoqi Chen², Kunze Huang¹, Xinghao Ding¹ and Yue Huang^{1†}

¹ School of Informatics, Xiamen University, China

² Department of Computer Science, The University of Hong Kong, China

{lytang, yuanyuxuan0908}@stu.xmu.edu.cn, cqchen1994@gmail.com, kzhuang@stu.xmu.edu.cn
{dxh, yhuang2010}@xmu.edu.cn

Abstract

Foundation models have made incredible strides in achieving zero-shot or few-shot generalization, leveraging prompt engineering to mimic the problem-solving approach of human intelligence. However, when it comes to some foundation models like Segment Anything, there is still a challenge in performing well on out-of-distribution data, including camouflaged and medical images. Inconsistent prompting strategies during fine-tuning and testing further compound the issue, leading to decreased performance. Drawing inspiration from how human cognition processes new environments, we introduce **SlotSAM**, a method that reconstructs features from the encoder in a self-supervised manner to create object-centric representations. These representations are then integrated into the foundation model, bolstering its object-level perceptual capabilities while reducing the impact of distribution-related variables. The beauty of SlotSAM lies in its simplicity and adaptability to various tasks, making it a versatile solution that significantly enhances the generalization abilities of foundation models. Through limited parameter fine-tuning in a bootstrap manner, our approach paves the way for improved generalization in novel environments. The code is available at github.com/lytang63/SlotSAM.

1. Introduction

1.1. Existing Studies and Limitations

The impressive capabilities of foundation models [8, 9, 15, 16, 20] in zero-shot learning are a significant factor in their growing prominence. Taking the segmentation foundation models as an example, their primary goal is to achieve strong performance in dense predictions on arbitrary images, with the Segment Anything Model (SAM) [9] being

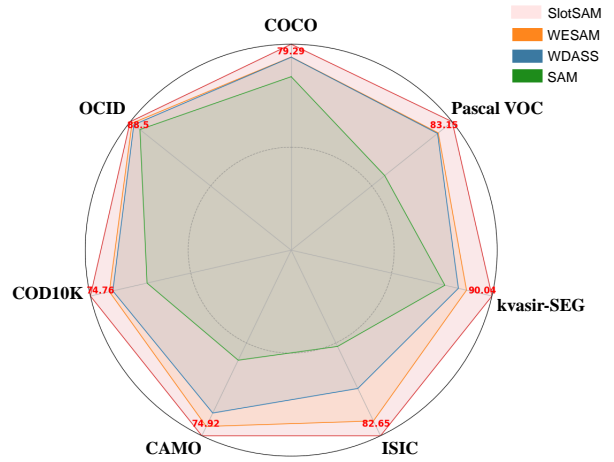


Figure 1. Performance comparison between SAM, WDASS, WE-SAM and SlotSAM across different downstream tasks under distribution shift and prompt shift.

a representative work. Despite SAM’s claimed robust zero-shot segmentation capabilities, distribution shift in challenging downstream tasks (e.g., medical imaging, camouflaged objects, low-quality images) undermines its advantages.

Enhancing SAM’s generalization and robustness on new data is a key focus. Fine-tuning is an intuitive method to adapt SAM to various downstream tasks. This may involve customizing a medical image-specific adapter [14] or integrating SAM as an additional supervisory branch in a semi-supervised segmentation framework for improved consistency learning [24]. However, these techniques require re-training on datasets with fine-grained annotations, often unavailable in real-world scenarios.

Recent research [11] has employed Stable Diffusion to enhance a subset of the SA-1B [9] dataset by generating adversarial instances, leading to improved performance of the SAM model, which requires unsustainable consumption of resources. Although this strategy constitutes a form of

*First two authors contributed equally.

†Corresponding author.

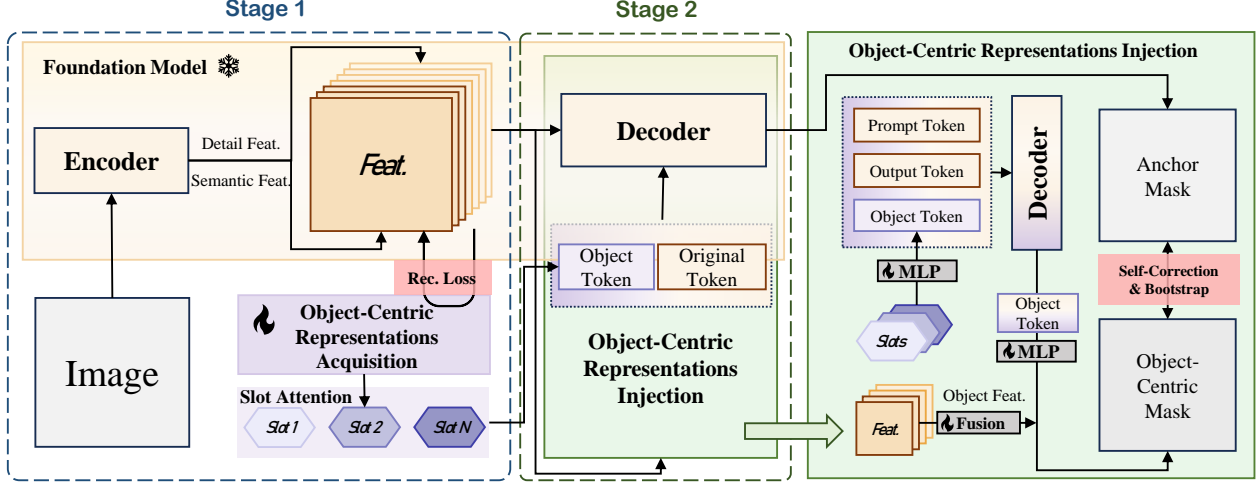


Figure 2. Overview of SlotSAM. Stage 1 is to obtain slots by reconstructing higher-order semantics. Stage 2 is to inject slots into the foundation model by nonlinearly combining them into object token and self-training. The whole process is task-independent.

model fine-tuning, its implementation in real-world scenarios remains challenging due to substantial computational resource consumption. WESAM [23] focuses on adapting the SAM by incorporating a frozen source model as an anchor. Under weak supervision, it utilizes LoRA [7] to fine-tune the model, thereby diminishing reliance on data and computational resources. However, WESAM’s enforcement of contrastive learning between different instances within images disrupts the semantic relationships among similar objects and can result in error accumulation.

1.2. Our Intuition and Insights

The poor performance of current foundation models in unknown environments can be attributed to two types of real-world shifts. The first is **distribution shift** [10, 19], which occurs when the data used for training (source domain) has a different distribution from the data encountered in downstream tasks during the actual application (target domain). The second is **prompt shift** [1, 25], where downstream tasks provide only coarse weak supervision instead of the fine-grained labels available in the source domain.

To address these challenges, we draw inspiration from the perceptual pipeline of human cognition in unfamiliar environments. We aim to simulate human-like intelligence [2] by abstracting the real world at the object level and injecting this capability into any foundation model. Object-centric learning [13] operates based on causal mechanisms that align with the physical world. By leveraging its combinatorial reasoning properties in scene comprehension, object-centric learning reduces reliance on domain-specific variables and enables more robust handling of out-of-distribution data.

Applying Slot-Attention [13], the core technology of object-centric learning, to unsupervised RGB pixel recon-

struction in foundation models lacks meaningfulness for three reasons. Firstly, the optimization objective of reconstructing the image itself lacks sufficient information for discerning real-world objects, potentially leading to degradation, as shown in Fig. 3. Secondly, training foundation models typically involve large-sized images, resulting in unacceptable resource overhead associated with Slot-Attention. Finally, the injection of object-centric representations compatible with foundation models and the enhancement of their object perception capabilities warrant careful consideration.

Considering the aforementioned factors, our objective is to redefine the reconstruction target of Slot-Attention as high-level features with stronger inductive biases. The image encoder of the foundation model effectively extracts high-level semantics for each object within the image, offering a uniform representation of the high-dimensional nature of the real world without being biased by pixel color reconstruction. High-quality object-centric representations, seamlessly integrated with existing tokens in most foundation models, can be considered as object tokens. During the forward process, object tokens can leverage the attention mechanism among tokens to access global image context, geometric region, semantic information, and mask regions. This significantly enhances the foundation model’s object perception capabilities with minimal fine-tuning parameters. As the entire process is unsupervised and reinforces the generalizability of the foundation model, relying on its exceptional feature representation, we define it as bootstrapping. Our contributions can be summarized as follows:

we introduce a task-agnostic approach for acquiring high-quality object-centric representations, enhancing the generalization capability of foundation models by incorporating object perception capabilities while keeping resource

consumption low.

2. Methodology

2.1. Preliminaries

Our original intention is to provide a way to inject object-centric representation perception capabilities into foundation models in a general sense. Therefore, the training process of the foundation models is not the focus of attention, so we do not differentiate between the optimization objectives of the original foundation models or the fine-tuned foundation models, modeling their loss functions as $\mathcal{L}_{\text{base}}$.

We chose the SAM as a representative foundation model for our research. SAM consists of three main components: the image encoder $\mathbf{z} = f(\mathbf{x}; \Theta)$, the prompt encoder $\mathbf{e} = g(\mathbf{p}; \Omega)$, and the mask decoder $h(\mathbf{z}, \mathbf{e}; \Phi)$. Inspired by [23], we used the universal optimization method as $\mathcal{L}_{\text{base}}$ for SlotSAM. We maintain three encoder networks, where for each input \mathbf{x} , we obtain \mathbf{x}_s and \mathbf{x}_w through strong augmentation and weak augmentation, respectively. \mathbf{x}_w is then processed by the anchor model $f(\mathbf{x}_w; \Theta^a)$ and the student model $f(\mathbf{x}_w; \Theta^s)$ to obtain \mathcal{M}^a and \mathcal{M}^s , while the teacher model $f(\mathbf{x}_s; \Theta^t)$ processes \mathbf{x}_w to obtain \mathcal{M}^t . \mathcal{M} represents the predicted mask. A generic teacher-student self-training loss can be defined as

$$\mathcal{L}_{\text{base}} = \mathcal{L}^{\text{dice}}(\mathcal{M}^{s/t}, \mathcal{M}^a) + \mathcal{L}^{\text{focal}}(\mathcal{M}^s, \mathcal{M}^t). \quad (1)$$

2.2. Object-Centric Representation Acquisition

Simply reconstructing RGB pixels allows Slot-Attention to achieve some effectiveness on synthetic datasets, but in the real world, RGB supervision signals are insufficient to represent objects and environments, making them prone to degradation, as shown in Fig. 3. Inspired by [17], object-centric representation requires a more well-trained semantic encoder, and fortunately, the encoder of the foundation model can provide rich semantic details.

The underlying logic of Slot-Attention is to reconstruct features through self-supervision, compressing high-dimensional, semantically rich, and unstructured object features into low-dimensional structured information in a bottleneck-like manner. Slots act as the bottleneck, retaining object-centric representation. Therefore, given the output feature $\mathbf{z} \in \mathbb{R}^{N \times D_z}$ from the encoder $f(\mathbf{x}; \Theta)$, and initializing a set of slots $\mathbf{s} \sim \mathcal{N}(\mathbf{s}; \boldsymbol{\mu}, \boldsymbol{\sigma}) \in \mathbb{R}^{K \times D_s}$, K is the number of slots, D_z and D_s represent the dimension of output feature and slot. We project them to dimensions by a linear transformation \mathcal{K}_β for slots and $\mathcal{Q}_\gamma, \mathcal{V}_\phi$ for \mathbf{z} , and the Slot-Attention is trained as $\text{update}(\mathbf{A}, \mathbf{v}) = \mathbf{A}^T \mathbf{v}$, where $\text{update}(\mathbf{A}, \mathbf{v}) = \mathbf{A}^T \mathbf{v}, A_{ij} = \frac{\text{attn}(\mathbf{q}, \mathbf{k})_{ij}}{\sum_{l=1}^K \text{attn}(\mathbf{q}, \mathbf{k})_{lj}}, \text{attn}(\mathbf{q}, \mathbf{k}) = \frac{e^{M_{ij}}}{\sum_{l=1}^N e^{M_{il}}}, \mathbf{M} = \frac{\mathbf{q} \mathbf{k}^T}{\sqrt{D_s}}$. The $\mathbf{q} = \mathcal{Q}_\gamma(\mathbf{z}) \in \mathbb{R}^{K \times D_s}, \mathbf{k} = \mathcal{K}_\beta(\mathbf{z}) \in \mathbb{R}^{N \times D_s}$, and

$\mathbf{v} = \mathcal{V}_\phi(\mathbf{z}) \in \mathbb{R}^{N \times D_s}$ denote the query, key and value vectors respectively. The query is a function of the slots. After optimizing T iterations using the Gated Recurrent Unit [3, 5] (GRU), the slots are passed through a slot-decoder to output the reconstructed feature $\hat{\mathbf{z}}$, minimizing the self-supervised reconstruction loss:

$$\mathcal{L}_{\text{rec}} = \|\hat{\mathbf{z}} - \mathbf{z}\|^2, \quad \hat{\mathbf{z}} = \text{slot-decoder}(\mathbf{s}). \quad (2)$$

$\hat{\mathbf{z}}$ is the weighted sum of each slots. Since each slot should be associated with a different object, each slot should be able to attend to specific spatial regions. Following the approach in [17], we employ an efficient MLP as a spatial broadcast decoder [22]. Each slot is broadcasted to several patches with the addition of positional encoding. The tokens for each slot are processed individually by the MLP, and after channel division, we obtain the reconstructed feature $\hat{\mathbf{z}}_k$ and the activation region α_k . The weighted feature representation $\hat{\mathbf{z}}$ for all slots after reconstruction is obtained by

$$\hat{\mathbf{z}} = \sum_{k=1}^K \hat{\mathbf{z}}_k \odot \mathbf{m}_k, \quad \mathbf{m}_k = \text{softmax}_k(\alpha_k). \quad (3)$$

2.3. Object-Centric Representation Injection

In the decoder of SAM, the predicted mask is obtained by performing element-wise multiplication between the Output Token $\mathcal{T}_{\text{out}} \in \mathbb{R}^{N_{\text{out}} \times D_{\text{out}}}$ and the mask feature. The accuracy of the mask is strongly correlated with the amount of information provided by the tokens. Therefore, as shown in Fig. 2, we innovatively design the object-centric representation stored in the slots to be the Object Token. This design is fully compatible with the original decoder architecture, and thanks to the attention mechanism, the Object Token can exchange information with other tokens. The Object Token can access the global image’s contextual information and geometric details. Furthermore, the existing \mathcal{T}_{out} can acquire more discriminative features related to objects, such as positional information and topological associations.

For each input \mathbf{x} , there is a corresponding set of slots \mathbf{s} . To avoid disrupting the optimization preference established by the decoder for existing tokens, $\mathbf{s} \in \mathbb{R}^{K \times D_s}$ is fed into an MLP for nonlinear combination to obtain the Object Token $\mathcal{T}_{\text{obj}} \in \mathbb{R}^{1 \times D_s}$, where $D_s = D_{\text{out}}$. In each attention layer, the Object Token performs self-attention calculations with other tokens and shares the same feed-forward layers to ensure consistent optimization direction of model.

As the \mathcal{T}_{obj} contains more deep semantic features and fewer detailed features, introducing local boundary details helps avoid boundary blurring for objects. Inspired by [8], We extract the detail features from the first attention block of the encoder. After applying transposed convolution, we

Method	COCO 2017			Pascal VOC			kvasir-SEG			ISIC			CAMO			COD10K			OCID		
	box	point	poly	box	point	poly	box	point	poly	box	point	poly	box	point	poly	box	point	poly	box	point	poly
SAM [9]	74.29	55.06	65.64	69.21	69.21	60.79	81.59	62.30	54.03	66.74	53.42	62.82	62.72	57.43	50.85	66.32	63.61	40.04	86.35	71.41	72.81
TENT [21]	78.21	52.99	71.51	80.24	74.97	65.03	82.47	61.84	62.97	71.76	53.46	67.12	71.24	59.59	60.29	69.36	61.94	43.36	87.77	66.61	77.53
SHOT [12]	75.18	58.46	69.26	79.80	74.26	63.38	82.30	63.76	61.34	71.99	55.99	66.86	71.61	62.78	58.72	69.09	65.25	42.38	88.06	74.39	76.25
TRIBE [18]	77.56	49.56	70.99	78.87	69.21	65.39	85.05	73.03	64.61	72.61	50.36	67.99	66.00	61.97	60.54	67.84	63.62	42.75	86.77	67.86	76.50
DePT [6]	71.00	37.35	63.27	74.09	42.99	59.94	81.91	52.06	61.55	78.43	46.79	72.75	55.44	33.07	48.63	59.32	34.06	35.51	82.00	56.52	70.92
WDASS [4]	77.29	60.55	70.19	80.12	76.15	66.98	84.01	63.78	64.78	74.23	55.63	67.84	71.25	63.39	62.29	71.42	65.61	43.93	87.68	77.13	76.70
WESAM [23]	77.32	60.5	70.77	80.27	74.15	66.72	85.47	75.23	67.40	80.01	62.12	75.36	73.42	65.55	62.90	71.93	70.55	45.87	88.09	80.14	77.41
Ours	79.29	60.99	75.48	83.15	77.23	70.77	90.04	81.96	79.64	82.65	66.21	78.72	74.92	68.95	71.09	74.76	72.46	48.86	88.50	81.35	79.54
improv.	+5.00	+5.93	+9.84	+13.94	+8.02	+9.98	+8.45	+19.66	+25.61	+15.91	+12.79	+15.90	+12.20	+11.52	+20.24	+8.44	+8.85	+8.82	+2.15	+9.94	+6.73
Supervised	81.50	69.77	73.39	81.23	76.98	71.32	85.89	77.54	81.64	81.62	79.81	80.26	79.17	77.01	67.12	78.06	78.44	64.90	91.24	89.22	79.23

Table 1. Comparison with SOTAs on **natural**, **medical**, **camouflaged object**, and **robotic** image datasets using **bounding box**, **sparse points**, and **coarse segmentation mask** prompts. The results of the baselines in the table are from [23].

add the detail feature with the semantic features to obtain fused object features \mathbf{z}^{obj} . Then, similar operations are performed, where the \mathcal{T}_{obj} is multiplied by the \mathbf{z}^{obj} to obtain the Object-Centric Mask \mathcal{M}^o .

Self-training networks may suffer from the problem of error accumulation due to incorrect predictions. Therefore, in the early stages of training, we fix the parameters of the anchor model (with \mathbf{x}_w as the input). The trained model is referred to as the object-centric model (with \mathbf{x}_s as the input). We use a simplified loss function in the style of \mathcal{L}_{base} to train the MLP and Fusion modules, in order to prevent significant bias in knowledge transfer:

$$\mathcal{L}^{dice}(\mathcal{M}^o, \mathcal{M}^a) + \mathcal{L}^{bce}(\mathcal{M}^o, \mathcal{M}^a). \quad (4)$$

In the later stages of training, we employ a bootstrap strategy. At the end of epochs where the model has improved its mIoU on the validation set, we directly copy the parameters of the object-centric model to the anchor model. Through this iterative process, we gradually complete the bootstrap of the foundation model.

3. Experiments

Quantitative analysis: As shown in Tab. 1 and Fig. 1, we evaluated SlotSAM on seven datasets and three prompt modalities. Astonishingly, SlotSAM outperforms existing methods by a large margin. SlotSAM narrows the gap on natural images with fully supervised fine-tuning and even surpassed fine-grained masking under point or poly prompts supervision. On medical images, our mIoU on the kvasir-SEG dataset exceeded 90% and remained performant even under poly prompts, surpassing WESAM [23] by 18.16%. On the most challenging dataset of camouflaged objects, we achieved an average improvement of over 3%.

Qualitative analysis: Fig. 4 compares the masks predicted by SlotSAM and existing SOTA methods. SlotSAM provides the most detailed predictions in regions with smaller pixel area occupancy, such as the junction of a horse’s hair and face, indicating its ability to capture the semantic correlations within the object and incorporate the acceptable boundaries into the object representation. Slot-

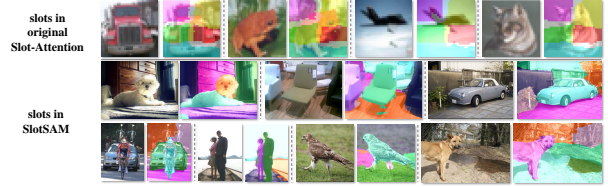


Figure 3. Comparison of the quality of the slots.

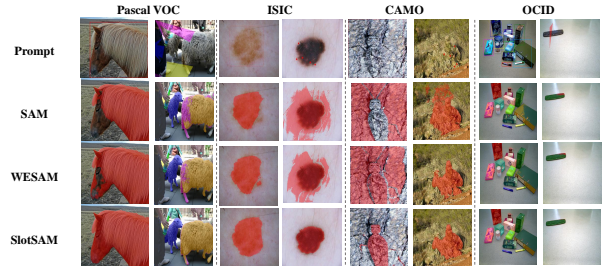


Figure 4. Comparison of the fineness of the predicted masks.

SAM provides higher semantic distinctiveness in ambiguous boundary areas, such as camouflaged objects and similar backgrounds, avoiding semantic confusion. This demonstrates that the distinctiveness among slots is transferred to the foundation model, enabling it to distinguish between different objects easily. Fig. 3 illustrates that SlotSAM can obtain non-degraded object-centric representations.

4. Conclusion and Discussion

We research the generalization of foundation models under distribution shift. A universal, concise approach is proposed to inject object-centric representation awareness into the foundation model, enabling it to focus on causal factors related to objects and achieve generalization. Building upon the framework of SAM, we propose SlotSAM, which can self-train in a bootstrapping manner without accessing the fine-grained label. The proposed method has undergone extensive evaluations in multiple datasets that cover four types of downstream tasks. The experimental results have demonstrated that SlotSAM has taken an important step toward robustly handling distribution shift and prompt shift.

In this work, we primarily focus on acquiring and injecting object-centric representations. Future research could explore differences in the distribution of slots, potentially enabling models to have more detailed awareness and it would be meaningful to utilize slots for controlled generative models.

References

- [1] Jameel Abdul Samadh, Mohammad Hanan Gani, Noor Hussein, Muhammad Uzair Khattak, Muhammad Muzammal Naseer, Fahad Shahbaz Khan, and Salman H Khan. Align your prompts: Test-time prompting with distribution alignment for zero-shot generalization. *Advances in Neural Information Processing Systems*, 36, 2024. 2
- [2] Collin Burns, Pavel Izmailov, Jan Hendrik Kirchner, Bowen Baker, Leo Gao, Leopold Aschenbrenner, Yining Chen, Adrien Ecoffet, Manas Joglekar, Jan Leike, et al. Weak-to-strong generalization: Eliciting strong capabilities with weak supervision. *arXiv preprint arXiv:2312.09390*, 2023. 2
- [3] Junyoung Chung, Caglar Gulcehre, KyungHyun Cho, and Yoshua Bengio. Empirical evaluation of gated recurrent neural networks on sequence modeling. *arXiv preprint arXiv:1412.3555*, 2014. 3
- [4] Anurag Das, Yongqin Xian, Dengxin Dai, and Bernt Schiele. Weakly-supervised domain adaptive semantic segmentation with prototypical contrastive learning. In *Proceedings of the IEEE/CVF Conference on Computer Vision and Pattern Recognition*, pages 15434–15443, 2023. 4
- [5] Rahul Dey and Fathi M Salem. Gate-variants of gated recurrent unit (gru) neural networks. In *2017 IEEE 60th international midwest symposium on circuits and systems (MWS-CAS)*, pages 1597–1600. IEEE, 2017. 3
- [6] Yunhe Gao, Xingjian Shi, Yi Zhu, Hao Wang, Zhiqiang Tang, Xiong Zhou, Mu Li, and Dimitris N Metaxas. Visual prompt tuning for test-time domain adaptation. *arXiv preprint arXiv:2210.04831*, 2022. 4
- [7] Edward J Hu, Yelong Shen, Phillip Wallis, Zeyuan Allen-Zhu, Yuanzhi Li, Shean Wang, Lu Wang, and Weizhu Chen. Lora: Low-rank adaptation of large language models. *arXiv preprint arXiv:2106.09685*, 2021. 2
- [8] Lei Ke, Mingqiao Ye, Martin Danelljan, Yu-Wing Tai, Chi-Keung Tang, Fisher Yu, et al. Segment anything in high quality. *Advances in Neural Information Processing Systems*, 36, 2024. 1, 3
- [9] Alexander Kirillov, Eric Mintun, Nikhila Ravi, Hanzi Mao, Chloe Rolland, Laura Gustafson, Tete Xiao, Spencer Whitehead, Alexander C Berg, Wan-Yen Lo, et al. Segment anything. In *Proceedings of the IEEE/CVF International Conference on Computer Vision*, pages 4015–4026, 2023. 1, 4
- [10] Pang Wei Koh, Shiori Sagawa, Henrik Marklund, Sang Michael Xie, Marvin Zhang, Akshay Balsubramani, Weihua Hu, Michihiro Yasunaga, Richard Lanus Phillips, Irena Gao, et al. Wilds: A benchmark of in-the-wild distribution shifts. In *International conference on machine learning*, pages 5637–5664. PMLR, 2021. 2
- [11] Bo Li, Haoke Xiao, and Lv Tang. Asam: Boosting segment anything model with adversarial tuning. In *Proceedings of the IEEE/CVF Conference on Computer Vision and Pattern Recognition*, pages 3699–3710, 2024. 1
- [12] Jian Liang, Dapeng Hu, Yunbo Wang, Ran He, and Jiashi Feng. Source data-absent unsupervised domain adaptation through hypothesis transfer and labeling transfer. *IEEE Transactions on Pattern Analysis and Machine Intelligence*, 44(11):8602–8617, 2021. 4
- [13] Francesco Locatello, Dirk Weissenborn, Thomas Unterthiner, Aravindh Mahendran, Georg Heigold, Jakob Uszkoreit, Alexey Dosovitskiy, and Thomas Kipf. Object-centric learning with slot attention. *Advances in neural information processing systems*, 33:11525–11538, 2020. 2
- [14] Jun Ma, Yuting He, Feifei Li, Lin Han, Chenyu You, and Bo Wang. Segment anything in medical images. *Nature Communications*, 15:1–9, 2024. 1
- [15] Alec Radford, Jong Wook Kim, Chris Hallacy, Aditya Ramesh, Gabriel Goh, Sandhini Agarwal, Girish Sastry, Amanda Askell, Pamela Mishkin, Jack Clark, et al. Learning transferable visual models from natural language supervision. In *International conference on machine learning*, pages 8748–8763. PMLR, 2021. 1
- [16] Baptiste Roziere, Jonas Gehring, Fabian Gloeckle, Sten Sootla, Itai Gat, Xiaoqing Ellen Tan, Yossi Adi, Jingyu Liu, Tal Remez, Jérémy Rapin, et al. Code llama: Open foundation models for code. *arXiv preprint arXiv:2308.12950*, 2023. 1
- [17] Maximilian Seitzer, Max Horn, Andrii Zadaianchuk, Dominik Zietlow, Tianjun Xiao, Carl-Johann Simon-Gabriel, Tong He, Zheng Zhang, Bernhard Schölkopf, Thomas Brox, et al. Bridging the gap to real-world object-centric learning. 2023. 3
- [18] Yongyi Su, Xun Xu, and Kui Jia. Towards real-world test-time adaptation: Tri-net self-training with balanced normalization. In *Proceedings of the AAAI Conference on Artificial Intelligence*, pages 15126–15135, 2024. 4
- [19] Rohan Taori, Achal Dave, Vaishaal Shankar, Nicholas Carlini, Benjamin Recht, and Ludwig Schmidt. Measuring robustness to natural distribution shifts in image classification. *Advances in Neural Information Processing Systems*, 33:18583–18599, 2020. 2
- [20] Hugo Touvron, Louis Martin, Kevin Stone, Peter Albert, Amjad Almahairi, Yasmine Babaei, Nikolay Bashlykov, Soumya Batra, Prajjwal Bhargava, Shruti Bhosale, et al. Llama 2: Open foundation and fine-tuned chat models. *arXiv preprint arXiv:2307.09288*, 2023. 1
- [21] Dequan Wang, Evan Shelhamer, Shaoteng Liu, Bruno Olshausen, and Trevor Darrell. Tent: Fully test-time adaptation by entropy minimization. In *International Conference on Learning Representations*, 2021. 4
- [22] Nick Watters, Loic Matthey, Chris P Burgess, and Alexander Lerchner. Spatial broadcast decoder: A simple architecture for disentangled representations in vaes. 2019. 3
- [23] Haojie Zhang, Yongyi Su, Xun Xu, and Kui Jia. Improving the generalization of segmentation foundation model under distribution shift via weakly supervised adaptation. In *Proceedings of the IEEE/CVF Conference on Computer Vision and Pattern Recognition*, pages 23385–23395, 2024. 2, 3, 4

- [24] Yichi Zhang, Yuan Cheng, and Yuan Qi. Semisam: Exploring sam for enhancing semi-supervised medical image segmentation with extremely limited annotations. *arXiv preprint arXiv:2312.06316*, 2023. [1](#)
- [25] Zhi-Hua Zhou. A brief introduction to weakly supervised learning. *National science review*, 5(1):44–53, 2018. [2](#)